ISSN 1063-7826, Semiconductors, 2020, Vol. 54, No. 10, pp. 1284–1289. © Pleiades Publishing, Ltd., 2020.

PHYSICS OF SEMICONDUCTOR DEVICES

Analysis of the Temperature Dependence of Diode Ideality Factor in InGaN-Based UV-A Light-Emitting Diode

P. Dalapati[a],*, N. B. Manik[a], and A. N. Basu[a]

[a] *Condensed Matter Physics Research Centre, Department of Physics, Jadavpur University, Kolkata, 700032 India*

**e-mail: pradipdalapati@gmail.com*

Received May 18, 2020; revised May 18, 2020; accepted June 9, 2020

Abstract—The temperature dependence of diode ideality factor in InGaN-based UV-A light-emitting diode has been investigated using the current–voltage characteristics at different temperatures. The obtained values of diode ideality factor are found to increase from 2.252 to 7.79 due to cooling down the device from 350 to 77 K. The evaluated values of diode ideality factors (even at high temperature) are greater than the expected values lying between unity to two. An attempt has been made to elucidate such greater value of diode ideality factor by existing theories as well as its effect on the diode characteristics.

Keywords: InGaN UV LED, diode ideality factor, tunnelling current, current crowding effect

DOI: 10.1134/S106378262010005X

1. INTRODUCTION

Recently, the ultraviolet (UV) light-emitting diodes (LEDs) based on gallium nitride (GaN) have drawn excessive attention owing to their potential applications in photocatalysis, water purification, sterilization, banknote identification, solid-state lighting (SSL), etc. [1, 2]. Also, InGaN-based commercial LEDs being easily available in the market, various problems associated with III-nitride semiconductor light-emitting materials have been reported to date [1–3]. But an interesting query regarding the typical values for the diode ideality factor n in InGaN-based LEDs needs to address properly, as this electrical parameter is important to decide the dominant current transport. According to Sah–Noyce–Shockley (SNS) theory, the value of n is between unity and two [4, 5]. On the contrary, for InGaN|GaN multiple quantum-well (MQW) blue LEDs it is reported that n is higher than two and it varies from 1.9 to 6.2 (for medium-bias regions) due to change in temperature from 300 to 100 K [6]. These values are found to be significantly different from those expected from SNS analysis. Although Achariya et al. [7] reported that the value of n could be up to 3 and it depends on the carrier generation and recombination processes within the space charge region (SCR) of the p–n junction, but however, that is not discussed in detail.

To account for the same, Shah et al. [8] developed a model considering the effect of metal contacts (i.e., the junctions behave like Schottky junctions) with the p–n junction. The metal contacts might be treated as the additional sources of diode ideality factors (factor).

In order to explain such high values of n, Masui et al. [4] have suggested an interesting experimental method to calculate n in InGaN-based LEDs where the effects of metal contact can be neglected. The authors have used the intensity of photoluminescence (PL) spectrum, particularly originating from the excited InGaN active region of LED, as a function of photo-excitation intensity keeping the external current to zero. In their measurements, they obtained the values of n of commercial LEDs lying between 1.1 and 2.4, whereas it took the values 2.5 and 5.3 calculated from the standard current–voltage—$I(V)$ characteristics. The obtained results from PL intensity for n were considerably smaller than the values calculated via $I(V)$ characteristics. Also, Chan et al. [9] reported an analytical formula for n from illuminated experimental data.

It is also reported that the current crowding effect (CCE) has an intense impact on n and likewise, whereas it needs to be conferred how they are correlated to each other [10, 11]. When the CCE occurs in LED then the distribution of current is not uniform and crowded at the specific region where the separation between n- and p-type metal contacts is minimum [10]. Mostly, the breakdown of LED followed the position where the current as well as the electric field were strongly concentrated. When the LED is operated in the medium-current domain (generally, 100 to 10 mA, the SCR prevails in the device characteristics), CCE is accountable for an abnormally high value of n (>2) [10]. Moreover, it is to be noted that CCE can moderate significantly the nature of charge carrier transport and carrier recombination in the device [12].

However, until now various research efforts are going on to establish a p–n diode structure where the value of n should be minimum. Zhu et al. [5] reported an exciting result on a significant decrease in n from 5.5 to 2.4 of GaInN|GaN MQW LEDs, when the existing quantum barriers (QBs) are serially doped by Si. These results indicate that in the active region, the band profiles play a leading role for the carrier transports and in this region, the unipolar hetero-junctions are the major parts to determine the value of n [5]. For the same purpose, Xu et al. [13] have fabricated InGaN-based blue LEDs with GaInN|GaInN polarization-matched MQW active regions and have got a lower value of n compared to the LEDs with conventional GaInN|GaN moderated polarization-mismatched MQW structure, and this lowering occurs mainly due to polarization matching and decreased electron leakage. Also, Lee et al. [14] measured the $I(V)$ characteristics of UV LEDs (wavelength = 310 nm) with different structures, namely, without electron blocking layer (EBL), with 4-nm EBL and 10-nm EBL, and reported the values of n which are 7.2, 6.9, and 5.5 for the respective structure. These results suggest that the value of n is closely related to the EBL thickness. However, from the above discussions, it is clear that n is an important parameter that is strongly associated with the nature of charge-carrier transport in such devices.

In the present investigation, we have measured the $I(V)$ characteristics of UV-A LED by standard technique, and from the slopes of a semi-logarithmic plot of the $I(V)$ data, we have extracted the values of n at different temperatures. Unlike the Shockley diode, n does not remain in the range between 1 and 2 and it is found to enhance nearly by a factor of 3.4 when the temperature is lowered to 77 from 350 K. In order to understand this alteration in the value of n and its temperature dependence, we employ different existing theoretical models. Our purpose is twofold. One is to look for a suitable formula involving n and temperature that may be used for the purpose of extrapolation over a large temperature range. Such a relation, if found, will be useful for different applications, particularly at low temperature. Secondly, from an analysis of the different models, we shall also try to identify the specific mechanism responsible for the high value of n which will give further insight into the device physics.

2. EXPERIMENTAL

One InGaN-based commercial UV-A LED has been chosen for the present investigation. The manufacturer of the LED is Bivar [15]. The peak wavelength and viewing angle of this tight tolerance (±2.5 nm) UV-A LED are 395 nm and 15°, respectively [15]. For the low-temperature characterisation, the device was inserted in the bath-type optical cryostat (BTOC). The surrounding area of LED inside the cryogen chamber was maintained to a pressure gradient of the order of 10^{-4} Torr with the help of high-vacuum pumping system to eliminate the dampness on the sample. After attaining the high vacuum, the cryogen chamber of BTOC was filled by the cryogen (liquid nitrogen) to produce low temperature. To measure temperature in the interval of 350 to 77 K, we used a K-type thermocouple. One end of the thermocouple was attached directly with the Cu sample holder (near to the sample) and another end was connected to a multimeter (Keithley 2000) to measure the generated thermo-emf in the thermocouple. $I(V)$ measurements at different temperatures were recorded on the Keithley 2400 source measure unit.

3. RESULTS AND DISCUSSION

The forward $I(V)$ characteristic in InGaN LED can be expressed by a standard diode equation as

$$I = I_S \exp\left(\frac{qV}{nKT} - 1\right). \quad (1)$$

The quantities I_S, q, K, and T represent the reverse saturation current, the electron charge, the Boltzmann constant, and the temperature, respectively.

The value of n can be estimated from the measured $I(V)$ data using the relationship given as

$$n = \frac{q}{KT}\left(\frac{qV}{d(\ln I)}\right). \quad (2)$$

The value of the slope $dV/d(\ln I)$ can be calculated from the linear portion of the forward biased semi-logarithmic $I(V)$ characteristic. The measured $I(V)$ characteristics at different temperatures for InGaN-based LED are shown in Fig. 1, plotted in semi-logarithmic scale.

The temperature dependence of n for the present device is shown in Fig. 2.

Figure 2 reveals that the value of n rises from 2.252 to 7.79 as the temperature decreases from 350 to 77 K. This result suggests that the temperature has a significant influence on n, which is inconsistent with the Shockley's equation for p–n junction diode. According to this model, n almost does not depend on temperature [16, 17]. It is mentioned in [18–21], the diffusion recombination current will dominate for the total diode current when the parameter n lies within 1 and 2; where n is very high (>2), tunnelling mechanism will prevail the diode current.

In order to get an appropriate formula for the $n(T)$ relation and in our search for an understanding of the current conduction mechanism in the device, we have used, in the following, three theoretical models and three empirical relations, and have compared their predictions vis-a-vis the experimental results.

To have a standard relationship between n and temperature, Achariya et al. [7] suggest a formula which is

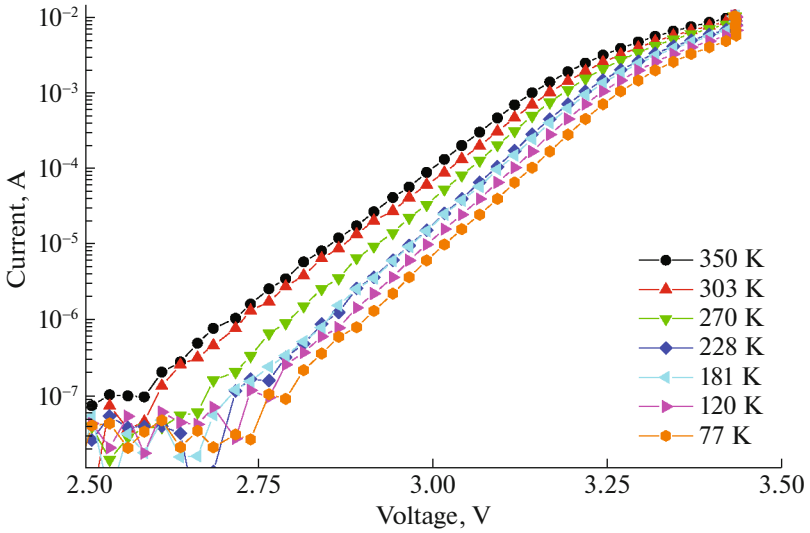

Fig. 1. Temperature-dependent $I(V)$ curves from 350 to 77 K. All the curves are plotted in semi-logarithmic scale.

similar to the form of band gap variation with temperature; it is given as

$$n = n(0) - \frac{\alpha_1 T^2}{T + \beta}, \quad (3)$$

where $n(0)$ is the diode ideality factor at 0 K and α_1 and β are some constants. The variation of n as a function of $T^2/(T + \beta)$ is shown in Fig. 3.

In Fig. 3, we have used the value of $\beta = 600$ K which is approximately the Debye temperature for GaN material [6]. In the temperature interval of 350 to 228 K, the temperature dependence of n has been found to agree well with the experiment with the corresponding values of $n(0) = 3.8$ and $\alpha_1 = 0.083$, respectively, whereas below this temperature, Eq. (3) does not hold good for this LED. It is also to be noted that for GaN device the value of α_1 is generally 7.7×10^{-4} [6] but in our case, it is too high. If we consider the band-gap narrowing effect (BGN), the value of α_1 may be changed [18] but this change should be less compared to the value obtained from Fig. 3.

Now it will be instructive to consider the Levine's model in order to understand the origin of the discrepancy between the prediction of Eq. (3) and experiment at low temperature. In this model, the ideality factor as a function of temperature in given by [17]

$$n = 1 + \frac{T_0}{T}, \quad (4)$$

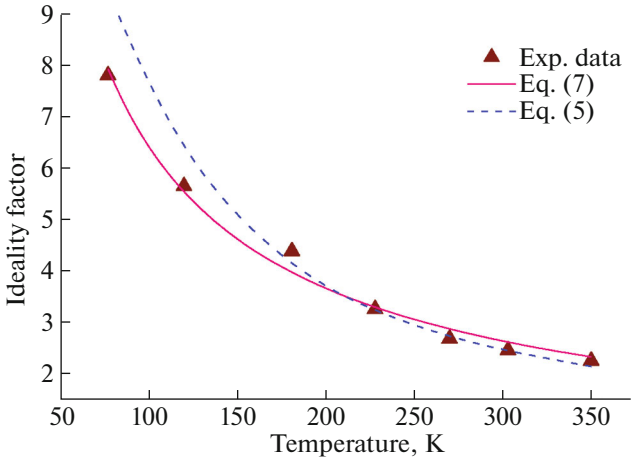

Fig. 2. Temperature-dependent diode ideality factor n of UV-A LED. The experimental points are designated by the solid up-triangle, whereas the numerical fits by dash line and continuous line according to Eqs. (5) and (7), respectively. According to Eq. (5), the value E_{00} equals to 62.53 meV.

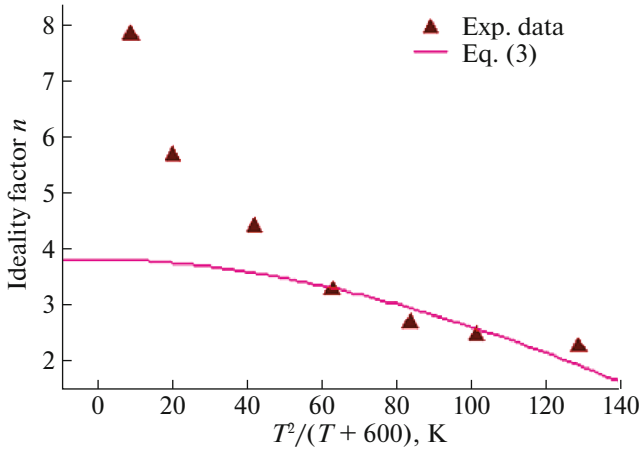

Fig. 3. Variation of n (solid up-triangle) as a function of $T^2/(T + \beta)$ for $\beta = 600$ K. The continuous line represents the numerical fit of Eq. (3).

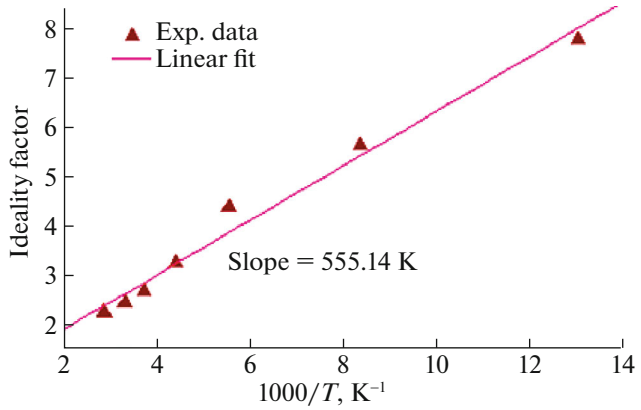

Fig. 4. Variation of n with $1000/T$.

with the pseudo-temperature T_0. It is to be mentioned that the magnitude of T_0 can vary with applied bias (fixed temperature) and it is closely related to the interfacial charge states. When the value of n lies between 1 and 2, the diffusion recombination current will flow in the diode and the value of T_0 should be almost zero [17]. On the other hand, the value of n larger than 2 directs the appearance of T_0 that supports for carrier dynamic through the hetero-junction. Furthermore, it is to be mentioned that it is controlled by interfacial states and thus tunnelling mechanism becomes effective [17]. If the interfacial states charge fluctuation at the hetero-junction increases we would get a larger value of T_0, which leads to temperature-dependent diode ideality factor. We fit our experimental data of InGaN-based LED, which is shown in Fig. 4, and we find that the value of T_0 is 555.14 K. Such large value of T_0 is the indication of lattice mismatch between InGaN|GaN hetero-junction [17].

Further inspection of Fig. 4 immediately reveals two things. First, the gradient of the straight line yields a finite and high value of the pseudo-temperature T_0. The high value of T_0 unambiguously points out that the diffusion of carriers followed by recombination according to SNS is inadequate to account for the current conduction in the device. Secondly, the overall qualitative agreement between the trends predicted by Eq. (4) and the experimental results throughout the entire range of temperature implies that it is the tunnelling of carriers that seem to be responsible for the diode current. However, the model does not provide any information about the origin and nature of this tunnelling phenomenon which we shall presently discuss later in this section.

The larger pseudo-temperature T_0 is not the only reason for the high value of n. To explain the origin of high n, an alternative model has been suggested by Shah et al. [8] in which they consider the GaN-based LED is a combination of rectifying unipolar hetero-junctions as well as metal-semiconductor contacts. In such multi-junction device, each junction has a certain value of n. Therefore, the externally measured value of n in such a device is an effective one. However, Shah et al. [8] used two different GaN-based p–n diode structures to evaluate the value of n. The calculated values of n for GaN diode structure and GaN p–n junction structure having 15 periods of p-type $Al_{0.2}Ga_{0.8}N|GaN$ super-lattice (SL) are 6.9 and 4.0, respectively. This result indicates that n can be significantly reduced by employing GaN|AlGaN SL structure as it leads to the formation of superior ohmic contacts than general bulk GaN p–n junction. Also, the temperature-dependent $I(V)$ measurements for the p–n junction with SL structure show decrease in the value of n at high temperature, namely, 473 K, due to the enhancement of p-type transport properties. At high temperature, contacts become less rectifying, leads for more ohmic behaviour. Thus, the overall n at high temperature will reduce due to the presence of metal–semiconductor junction. More precisely, our interest is to know how and how much the property of LED changes due to the presence of metal-semiconductor junction. For metal–semiconductor junction, we must treat the variation of n as for Schottky diode.

Next, in order to understand the underlying physics of the carrier transport mechanism of such multi-junction LED and how it is changed with ambient temperature, we consider two transport models, used in [22, 23]. In the case of first model, tunnelling enhanced interface recombination (TEIR), we can consider an interface with the higher population of electrons than the free holes, and for the second model, tunnelling enhanced bulk recombination (TEBR), the correction factor for the improvement of recombination by tunnelling process is related to the local band bending that can influence the recombination processes via differently distributed recombination centers (details of these models are described in [22, 23]). We have employed these two models in our study for a quantitative examination of experimental results, which will ultimately assist to decide the dominant carrier transport and recombination mechanisms in the device.

According to TEIR model, n can be expressed by the following expression

$$n = \frac{E_{00}}{kT}\coth\left(\frac{E_{00}}{kT}\right), \tag{5}$$

where $E_{00} = (q\hbar/2)[N/m^*\varepsilon_s]$ (N, m^*, and ε_s represent the semiconductor doping concentration, the effective tunnelling mass, and the semiconductor's dielectric constant, respectively) is the characteristic tunnelling energy [23]. The theoretical fit of Eq. (5) is shown in Fig. 2. We obtained the value of E_{00} from the fit as 62.53 meV for the present device.

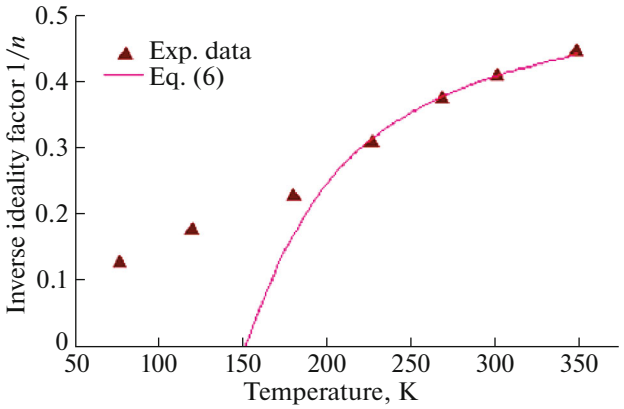

Fig. 5. A plot of inverse diode ideality factor $1/n$ versus temperature. The continuous line shows the numerical fit according to Eq. (6) where E_{00} equals to 21.12 meV.

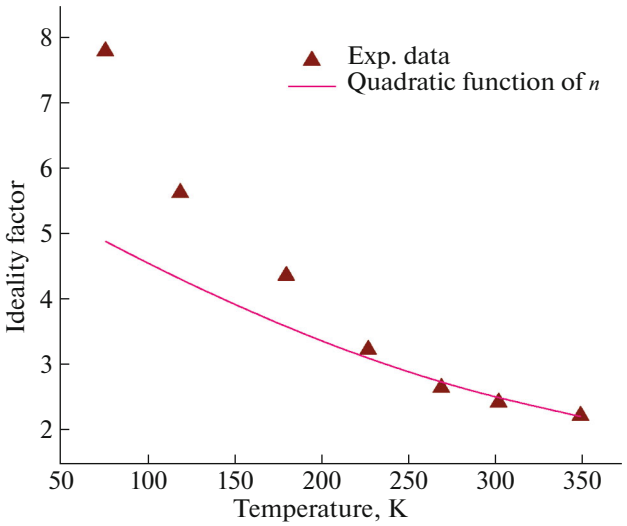

Fig. 6. n versus T curve. The solid up-triangle indicates the experimental points. Continuous line stands for the quadratic function $n = 6.11 - 0.017T + 1.7 \times 10^{-5} T^2$.

On the other hand, if we consider TEBR then n can be written as

$$\frac{1}{n} = \frac{1}{2}\left(1 - \frac{E_{00}^2}{3(kT)^2} + \frac{T}{T^*}\right), \quad (6)$$

where T^* is the characteristic temperature. To reproduce the obtained result by Eq. (6), we plot inverse n with temperature which is shown in Fig. 5 along with the numerical fit.

From Fig. 5, we obtained the value of E_{00} of 21.12 meV although the curve is not well fitted below 181 K.

The theoretical curves by Eqs. (5) and (6) are shown in Figs. 2 and 5, respectively. All the used best fit parameter values are also mentioned in the corresponding legends. It is distinctly clear that TEBR model can be used to interpret the experimental data at above 181 K for the present device. However, Eq. (5) based on TEIR model reproduces the obtained result for the temperature dependence of n with a single adjustable parameter E_{00}. The numerical fit of Eq. (5) implies that tunnelling significantly contributes to the recombination process via interface states for the investigated device.

In another effort, Zhang et al. [24] have tried to interpret their result by fitting a quadratic function. We have reproduces the data by using a quadratic function $n = 6.11 - 0.017T + 1.7 \times 10^{-5} T^2$, which is shown in Fig. 6.

The quadratic function fitted our result up to 228 K as shown in Fig. 6 by a continuous line, which indicates the variation of band gap energy with temperature is linear within the temperature interval of 350 to 228 K for the present device. The Varshni equation for band gap in this temperature range may be treated as $E_g(T) \approx E_{g,\,228} - \alpha_i(T - 228)$ with $E_{g,\,228}$ being the band gap energy at 228 K and α_i is a constant having a positive value. However, at low temperature below 228 K, the extrapolated curve due to the quadratic function is found to deviate strongly from the experiment. This characteristic feature of the bang gap variation with temperature at a high temperature (>228 K) justifies why a band structure type formula given by Eq. (3) has successfully reproduced experimental results at high temperature regime (see Fig. 3). It is also interesting to note that both the formulae agree with observation till 228 K and do not hold good below this temperature.

Finally, we try to fit the $n - T$ data by an empirical relation suggested by us [25, 26] in connection with some InGaN LEDs. The relation is given by

$$n = \frac{A}{T^p}, \quad (7)$$

with two adjustable temperature-insensitive parameters A and p. With the value of $A = 265$ and $p = 0.8$, Eq. (7) approves fairly well with observation till 77 K (see Fig. 2).

A closer analysis of the results of calculation of $n - T$ relations evidently indicates that Eq. (5) is distinctly superior to other relations on two counts. First, it is only one which reproduces the entire trend of data with a single adjustable parameter. Although nearly comparable are the predictions of Eqs. (5) and (7), a scrutiny of Fig. 2 reveals that there is a deviation from the prediction of Eq. (7) from the experiment at high temperature for that of Eq. (5) at lower temperature. Secondly, unlike that of Eq. (5) we are at present unable to provide any direct physical significance of the parameters A and p occurring in Eq. (7). On the other hand, the only parameter E_{00} in Eq. (5) is the characteristic tunnelling energy that has direct physical significance. Additionally, an inspection of the terms in the expression for E_{00} immediately exposes that it is inversely related to the square root of the

effective tunnelling mass of carriers solely responsible for the tunnelling current. Even it is also possible to identify the nature of carriers by evaluating the value of m^* from Eq. (5) by knowing the values of N and the ε_s.

It is also surmised that the remaining disagreement between prediction of Eq. (5) and experiment at low temperature may significantly improve, if we include the effect of finite width of SCR as we have already noted in our previous work [23]. Both the above points we intend to investigate in future communication.

4. CONCLUSIONS

The investigation of n at various temperatures and its quantitative analysis are important to know the dominant current transport mechanism, the major recombination pathway inside the p–n junction device as well as the temperature-dependent performance of the device. For the present UV-A LED, the gradual improvement of n with lowering of temperature suggests that the tunnelling process gradually becomes significant in the lower temperature region.

According to Levine's model, the fact that the data on n versus T approximately fall on a straight line curve and the high value of pseudo-temperature T_0 as 555.14 K having the dimension of temperature indicate the dominance of tunnelling phenomenon. Further, the change in ratio of the pseudo-temperature and the device temperature that is the temperature of experiment from about only a factor of 2 to nearly 7, due to the change in temperature from 350 to 77 K is a rough measure of the increase in the tunnelling contribution to conduction current with lowering of temperature. Next, we try to focus on the issue of the metal contact effects in such a device. For this purpose, the experimental results are analysed by employing TEIR and TEBR transport models. The predictions of TEIR model show a distinct preference for the present device as it reproduces the temperature dependence of n quite better than TEBR transport model. The typical temperature dependence at low temperature may also be associated with the position of Fermi level as well as the position-dependent trap states in the forbidden gap. Moreover, the temperature stress can modify the conduction mechanism of the device significantly as the Fermi level is highly temperature-sensitive.

FUNDING

We acknowledge the Defence Research Development Organization (DRDO), India, for financial support.

CONFLICT OF INTEREST

We have no conflict of interest.

REFERENCES

1. Y. Li, J. Lan, W. Wang, Y. Zheng, W. Xie, X. Tang, D. Kong, Y. Xia, Z. Lan, R. Li, X. He, and G. Li, Opt. Express **27**, 7447 (2019).
2. A. E. Aslanyan, L. P. Avakyants, P. Y. Bokov, and A. V. Chervyakov, Semiconductors **53**, 477 (2019).
3. P. Dalapati, N. B. Manik, and A. N. Basu, Opt. Quant. Electron. **52**, 54 (2020).
4. H. Masui, S. Nakamura, and S. and P. Den Baars, Appl. Phys. Lett. **96**, 073509 (2010).
5. D. Zhu, J. Xu, A. N. Noemaun, J. K. Kim, E. F. Schubert, M. H. Crawford, and D. D. Koleske, Appl. Phys. Lett. **94**, 081113 (2009).
6. D. W. Yan, H. Lu, D. J. Chen, R. Zhang, and Y. D. Zheng, Appl. Phys. Lett. **96**, 083504 (2010).
7. Y. B. Acharya and P. D. Vyavahare, Solid State Electron. **43**, 645 (1999).
8. J. M. Shah, Y. L. Li, T. Gessmann, and E. F. Schubert, J. Appl. Phys. **94**, 2627 (2003).
9. D. S. H. Chan and J. C. H. Phang, IEEE Trans. Electron. Dev. **34**, 286 (1987).
10. G. Kim, J. H. Kim, E. Park, and B. G. Park, J. Semicond. Tech. Sci. **14**, 588 (2014).
11. V. K. Malyutenko, S. S. Bolgov, and A. D. Podoltsev, Appl. Phys. Lett. **97**, 251110 (2010).
12. C. De Santi, D. Monti, P. Dalapati, M. Meneghini, G. Meneghesso, and E. Zanoni, in *Light-Emitting Diodes*, Ed. by J. Li and G. Q. Zhang, Vol. 4 of *Solid State Lighting Technology and Application Series* (Springer, Cham, 2019), p. 397. https://doi.org/10.1007/978-3-319-99211-2_11
13. J. Xu, M. F. Schubert, A. N. Noemaun, D. Zhu, J. K. Kim, E. F. Schubert, M. H. Kim, H. J. Chung, S. Yoon, C. Sone, and Y. Park, Appl. Phys. Lett. **94**, 011113 (2009).
14. K. B. Lee, P. J. Parbrook, T. Wang, J. Bai, F. Ranalli, R. J. Airey, and G. Hill, Phys. Status Solidi B **247**, 1761 (2010).
15. https://docs-emea.rs-online.com/webdocs/0e77/0900766b80e77d25.pdf. Accessed August 24, 2019.
16. C. T. Sah, R. N. Noyce, and W. Shockley, Proc. IRE 45, 1228 (1957).
17. C. H. Li, C. K. Wang, W. Y. Chen, W. T. Wang, C. W. Hung, C. C. Ke, J. C. Wang, H. T. Shen, and T. E. Nee. http://research.cgu.edu.tw/ezfiles/14/1014/img/651/96-B-32.pdf. Accessed April 12, 2019.
18. P. Dalapati, S. Maity, N. B. Manik, and A. N. Basu, Front. Optoelectron. **7**, 501 (2014).
19. C. Mi, L. Wang, J. Jin, Z. Hao, Y. Luo, C. Sun, Y. Han, B. Xiong, J. Wang, and H. Li, Appl. Phys. Express **12**, 032002 (2019).
20. A. B. M. H. Islam, D. S. Shim, and J. I. Shim, Appl. Sci. **9**, 871 (2019).
21. M. Lee, H. Lee, K. M. Song, and J. Kim, Nanomaterials **8**, 543 (2018).
22. V. Nadenau, U. Rau, A. Jasenek, and H. W. Schock, J. Appl. Phys. **87**, 584 (2000).
23. P. Dalapati, N. B. Manik, and A. N. Basu, Cryogenics **65**, 10 (2015).
24. Y. Zhang, M. Ding, D. Zhao, H. Huang, L. Huang, Y. Lin, D. Bian, B. Zhang, and Y. Cai, IEEE Trans. Elect. Dev. **65**, 564 (2018).
25. P. Dalapati, N. B. Manik, and A. N. Basu, Opt. Quant. Electron. **49**, 265 (2017).
26. P. Dalapati, N. B. Manik, and A. N. Basu, J. Electron. Mater. **45**, 2683 (2016).